ELSEVIER

Journal of Molecular Catalysis A: Chemical 176 (2001) 227–246

JOURNAL OF MOLECULAR CATALYSIS A: CHEMICAL

www.elsevier.com/locate/molcata

The synergism of cadmium on the catalytic activity of Cd–Cr–O system II. Ethanol decomposition, catalysts reducibility, and in situ electrical conductivity measurements

B.M. Abu-Zied*, A.M. El-Awad

Chemistry Department, Faculty of Science, Assiut University, 71516 Assiut, Egypt

Received 24 February 2001; accepted 6 June 2001

Abstract

In this paper, the conversion (dehydration/dehydrogenation) of ethanol over a series of chromia as well as cadmium/chromia catalysts calcined in the 400–1000°C temperature range has been studied. The reaction was performed in a fixed-bed reactor at atmospheric pressure and in the 150–400°C temperature range using nitrogen as a carrier gas. The reaction products were ethane, ethylene, and acetaldehyde together with trace amounts of ethyl acetate. The cadmium-containing catalysts, especially those calcined at 400 and 500°C, showed higher dehydrogenation activity. This trend was attributed to the catalyst reducibility, which was correlated with the presence of chromate ions. Such ions enhance the reduction of cadmium ions to zerovalent cadmium. Catalysts reducibility was checked by means of EtOH-temperature-programmed reduction (TPR), XRD, and FT-IR analyses. Moreover, in situ electrical conductivity measurements during alcohol admission were carried out. A good parallelism was found between the catalyst activity and its reducibility. In this way, the presence of Cd^0–Cr_2O_3 mixture, as a result of cadmium chromate reduction, showed a synergistic effect towards ethanol conversion as well as acetaldehyde selectivity. This effect was ascribed to the formation of donor–acceptor pairs as a consequence of Cd^0–Cr_2O_3 mixture formation.

Keywords: Synergism; Catalyst reduction; Ethanol decomposition; Cadmium chromate; Cadmium chromite; Spinels; Chromium(III) oxide

1. Introduction

Alcohol conversion considered as a model test reaction of acid–base/redox properties of many catalysts. Meanwhile, such reactions produce a variety of products that have a vital industrial importance [1]. Among several families of catalysts, noble metal-based materials [2–4], transition metal oxides [5–16], solid solutions and spinels [17–19], molybdates [20,21], perovskites [22], zeolites [23,24], and heteropoly compounds [25–31] showed an interesting activity features. Correlations between acid–base properties and catalytic activity, selectivity, and mechanism have been emerged as a result of these studies. Alcohols dehydrogenation products (aldehydes and ketones) are preferentially formed on basic catalysts, while the dehydration products (olefins and ethers) are favored when acidic sites are present [5,9,16,17,25]. With regard to the reaction mechanism, one of the widely

* Corresponding author. Tel.: +20-88-412107; fax: +20-88-342708.
E-mail addresses: babuzied@aun.eun.eg (B.M. Abu-Zied), el-awad@aun.eun.eg (A.M. El-Awad).

1381-1169/01/$ – see front matter
PII: S1381-1169(01)00263-1

accepted mechanisms of alcohols conversion over metal oxides [5] and spinels [19] involves: (i) adsorption and activation of the alcohol on active metal site, and (ii) decomposition of the alkoxide intermediate to form the reaction products.

It seems important to stress that not only the acid–base properties govern the activity and selectivity of a given catalyst towards alcohol conversion, other factors operate simultaneously, viz. structural and electronic features of the catalyst as well as its reducibility. Focusing our attention to the metal oxide systems and with regard to the influence of structural effects, studies showed that some metal oxides, e.g. lanthanum oxide [32], does not seem to be stable enough during its usage as a catalyst, since the presence of carbon dioxide and water, various carbonates and hydroxycarbonate compounds are easily formed. Moreover, formation of phases like $FeVO_4$ [19], $AgCrO_2$ [2], and $CuLa_2O_4$ [33] during their corresponding mixed oxides pretreatment can also lead to significant deactivation. On the other hand, it was reported [34] that the presence of supported physical mixture of CuO and Cu metal leads to a synergic effect towards the selective dehydrogenation of isopropanol. In agreement, McCabe and Mitchell [35] noticed that bimetallic mixture of Pd and Ag supported on alumina exhibits also a synergic effect during ethanol oxidation than the single component catalysts. As for the selectivity behavior, the subsequent literature contains an interesting report [36] that deposition of Cu^0 in monolayer amount onto the $(1\,0\,\bar{1}\,0)$ face of a single crystal of zinc oxide eliminated the dehydration activity, thus leaving the surface selective for ethanol dehydrogenation.

Regarding the electrical properties of the catalysts, Bevan et al. [37] suggested that chromium oxides are oxygen excess or p-type semiconductors, Weller and Voltz [38] and others [39] have shown that chromium oxides are p-type semiconductors in oxygen, but they become n-type in pure hydrogen due to the partial reduction of high valent states on the surface to Cr(II) ions. On MoO_3 [40], it was observed that an increase in the n-type conductivity increases isopropanol dehydration and as soon as the oxide becomes p-type, the activity drastically falls. Thus, 2-propanol dehydration on this catalyst is an acceptor or n-type reaction according to Wolkenstein nomenclature [41].

There have been various reports concerning the catalyst reducibility, and attempts have been made to relate the alcohol conversion activity with catalyst reducibility. Recently [22] and based on H_2-temperature-programmed reduction (TPR), it was shown that selective dehydrogenation of benzyl alcohol over a series of catalysts adopting the perovskite structure increases with the decrease in the temperature of maximum uptake of hydrogen. Concurrent with this ethanol dehydrogenation on reduced Cu supported on SiO_2 and ZrO_2 showed that [9] when the catalyst was reduced to metallic copper, the dehydrogenation of ethanol took place rapidly. No reactions occurred over unreduced catalysts or supports. This strongly supports the idea that alcohol dehydrogenation occurred over metallic copper surfaces. More recently [2] and with the aid of EtOH-TPR experiments, we showed that silver-chromate catalyst is reduced by hydrogen generated via ethanol dehydrogenation which was led to the formation of Ag^0–Cr_2O_3 mixture. Such mixture exhibited high activity towards ethanol decomposition in nitrogen and air atmospheres.

In part I of this work [42], we established the main structural features of the calcination products of chromia as well as cadmium/chromia catalysts. In addition, the electrical conductivity of these systems was also investigated. In this second part, we report the results of the catalytic activity measurements of both systems toward ethanol decomposition. Moreover, due to the lack of information on the modifications undergone by the cadmium/chromia catalysts over a long period or reaction with ethanol, particular attention was paid to study such structural changes. To achieve this, different techniques have been employed, viz. FT-IR, XRD, and EtOH-TPR. Finally, we have also investigated the electrical conduction properties of cadmium/chromia catalysts in ethanol vapor atmosphere.

2. Experimental

2.1. Materials

Analytical grade chemicals were used. Chromia and cadmium/chromia parents were prepared as described previously [42]. The two starting materials were calcined, for 5 h, in air atmosphere in the 400–1000°C temperature range. In addition, a sample of cadmium

oxide was prepared by thermal decomposition of cadmium carbonate, for 5 h, in air at 500°C. For simplicity, the catalysts will be referred to by abbreviations Cd-*x*, Cr-*x*, and Cd/Cr-*x* for cadmium, chromia, and cadmium/chromia catalysts, respectively, where *x* stands for the calcination temperature.

2.2. Apparatus and techniques

Ethanol decomposition was carried out in a flow system using nitrogen as a carrier gas. The catalytic runs were done by using a conventional fixed-bed continuous flow reactor made of Pyrex glass with i.d. of 15 mm. The temperature of the catalyst bed was measured with the help of a thermocouple placed in the center of the catalyst bed. The temperature was adjusted using a Cole–Parmer temperature controller (type Digi Sense). Before each catalytic run, the catalysts (0.3 g held in place between two glass wool plugs) were initially activated at 300°C for 2 h, then cooled to the reaction temperature. The reciprocal space velocity (*W*/*F*) was changed by changing the weight of the catalyst charged into the reactor. The reactant vapor was introduced by passing the carrier gas flow through a saturator containing the liquid ethanol. The molar feed rate was 3.85 mmol h^{-1}. The reactor effluent was sampled and analyzed by Shimadzu 14-A gas chromatograph. All experimental runs were taken under steady-state conditions. Identification of the reaction products was carried out by collecting a portion of the reactor effluent in a sampling flask, then analyzing it by using JEOL JMS 600 GC–MS spectrometer. The products identified were ethane, ethylene, acetaldehyde, and ethyl acetate.

TPR experiments by ethanol (EtOH-TPR) were performed using the thermogravimetric analyzer (TA thermal analyst 2000) with about 10 mg catalyst loaded in the pan. Prior to reduction, the catalyst was preheated by heating at 400°C for 30 min in nitrogen atmosphere at a flow rate of 100 cm^3 min^{-1}, followed by cooling to the desired temperature. Isothermal measurements were obtained by admitting the alcohol vapor using nitrogen carrier at fixed temperature, whereas non-isothermal measurements were obtained by introducing the alcohol vapor whilst the catalyst suffers from a continuous heat treatment (10°C min^{-1}).

Selected catalysts were re-characterized at the end of the catalytic runs by means of XRD, FT-IR, surface area measurements, and soluble Cr^{6+} determinations. The measuring procedures were reported in part I of this work [42].

2.3. In situ electrical conductivity

The variation of the electrical conductivity occurring when the cadmium/chromia catalysts were exposed to ethanol vapor were measured at 300°C. The measuring procedure is reported elsewhere [18].

3. Results and discussion

Ethanol decomposition was used to prove the reactivity of cadmium/chromia catalysts in comparison with the relevant calcined chromia catalysts. The variation of the ethanol conversion percentage with reaction temperature over Cr-*x* and Cd/Cr-*x* catalysts is shown in Figs. 1 and 2, respectively. The most important features emerge from these two figures are as follows: (i) the activity of both series of catalysts became already measurable at around 200°C; (ii) the activity of Cr-*x*, Cd/Cr-400, and Cd/Cr-500 catalysts increases smoothly with the temperature. On the other hand, the activity of the catalysts composed of chromite spinel, i.e. Cd/Cr catalysts calcined in the 600–1000°C temperature range, passes through a maximum; (iii) the activity of Cr-*x* catalysts declines with increasing the calcination temperature; (iv) it is

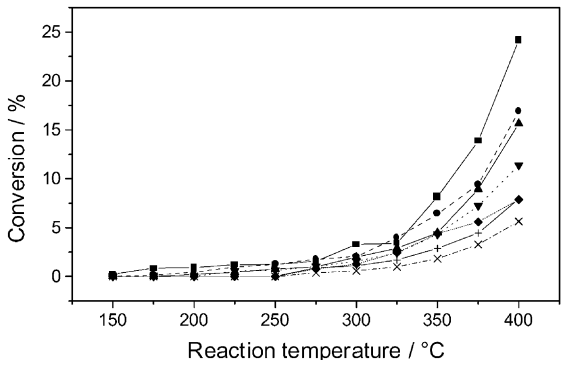

Fig. 1. Variation of the conversion percentage of ethanol as a function of the reaction temperature for the catalysts: Cr-400 (■); Cr-500 (●); Cr-600 (▲); Cr-700 (▼); Cr-800 (◆); Cr-900 (+); Cr-1000 (×).

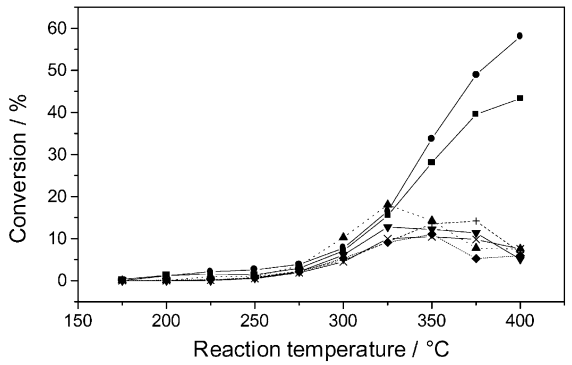

Fig. 2. Variation of the conversion percentage of ethanol as a function of the reaction temperature for Cd/Cr-catalysts calcined at: 400°C (■); 500°C (●); 600°C (▲); 700°C (▼); 800°C (◆); 900°C (+); 1000 (×).

evident that Cd/Cr-400 and Cd/Cr-500 catalysts show a higher activity patterns compared to the rest of the catalysts in both series. Meanwhile, Cd/Cr-500 catalyst is more active than Cd/Cr-400 one. These two facts will be discussed latter.

Regarding the reaction products, acetaldehyde, ethylene, and ethane were the main reaction products detected on both series. In addition, a trace amount of ethyl acetate (<1%) was also detected. Figs. 3 and 4 give the yield variation of the main products with reaction temperature of Cr-*x* and Cd/Cr-*x* catalysts, respectively. The products yield depends on catalyst type, whether it is Cr or Cd/Cr, also on both the reaction and the calcination temperatures. Chromia catalysts show a higher yield of ethylene, even at low conversions, than the relevant cadmium/chromia ones. Dehydration of alcohols is a characteristic reaction on acidic sites of transition metal oxides [5,43]. Thus, ethylene formation indicates the presence of a higher acidic sites on the Cr-*x* catalysts, which is corroborated by the formation of higher ethane selectivity than the relevant Cd/Cr-*x* catalysts, as it will be discussed latter. The maxima observed for the 600–1000°C calcined catalysts in Cd/Cr-*x* series (Fig. 2) is determined by the behavior of the main product, acetaldehyde, the yield of which reaches an analogous maxima at 325–350°C temperature range. Meanwhile, the yields of ethylene and ethane increase smoothly with the reaction temperature. The higher dehydrogenation activity of Cd/Cr-*x* catalysts compared to Cr-*x* ones suggests a higher basicity of the former catalysts than the latter ones.

As far the selectivity behavior of the dehydrogenation product in ethanol conversion is concerned, Fig. 5a and b, respectively, shows the variation of acetaldehyde selectivity with the conversion percentage of the most active catalysts in chromia and cadmium/chromia series. Two interesting observations were raised here. Firstly, the trend of variation of acetaldehyde selectivity with the conversion is the same for the individual catalysts in both series. Secondly, as the conversion increased as a result of raising the reaction temperature, a drop in acetaldehyde selectivity is observed for Cr-*x* catalysts. On the other hand, a gradual decrease in acetaldehyde selectivity is evident on Cd/Cr-400 and Cd/Cr-500 catalysts reaching, respectively, values of 76% at 43% conversion level and 73% at 58% conversion level. Thus, the selectivity patterns confirm the higher dehydrogenation activity of cadmium-containing catalysts. In agreement, Fahim et al. [44], working on the decomposition of isopropanol over calcined chromia catalysts, reported that increasing the percentage of doping of chromia with either Cd^{2+} or Ce^{4+} ions from 0.5 up to 10% (atomic ratio) is accompanied by an increase in the dehydrogenation reaction rate and a decrease in the surface Cr^{6+} ions. Moreover, the same authors showed that the maximum dehydrogenation activity occurs for the 10% Cd-doped catalyst previously calcined at 350°C.

Reviewing the literature revealed that there are four routes for alkanes production from primary alcohols.

1. The first is essentially an ether disproportionation reaction presumably mediated by surface adsorption [5]:

$$(C_2H_5)_2O \rightarrow CH_3CHO + C_2H_6 \uparrow \quad (1)$$

2. The second alternative is a reaction involving hydrogen generated by parallel dehydrogenation reaction [5] according to

$$(C_2H_5)_2O + 2H_2 \rightarrow 2C_2H_6 \uparrow + H_2O \quad (2)$$

3. The third route involves the reaction of hydrogen, formed via alcohol dehydrogenation, with an alcohol molecule [22] as follows:

$$C_2H_5OH + H_2 \rightarrow C_2H_6 \uparrow + H_2O \quad (3)$$

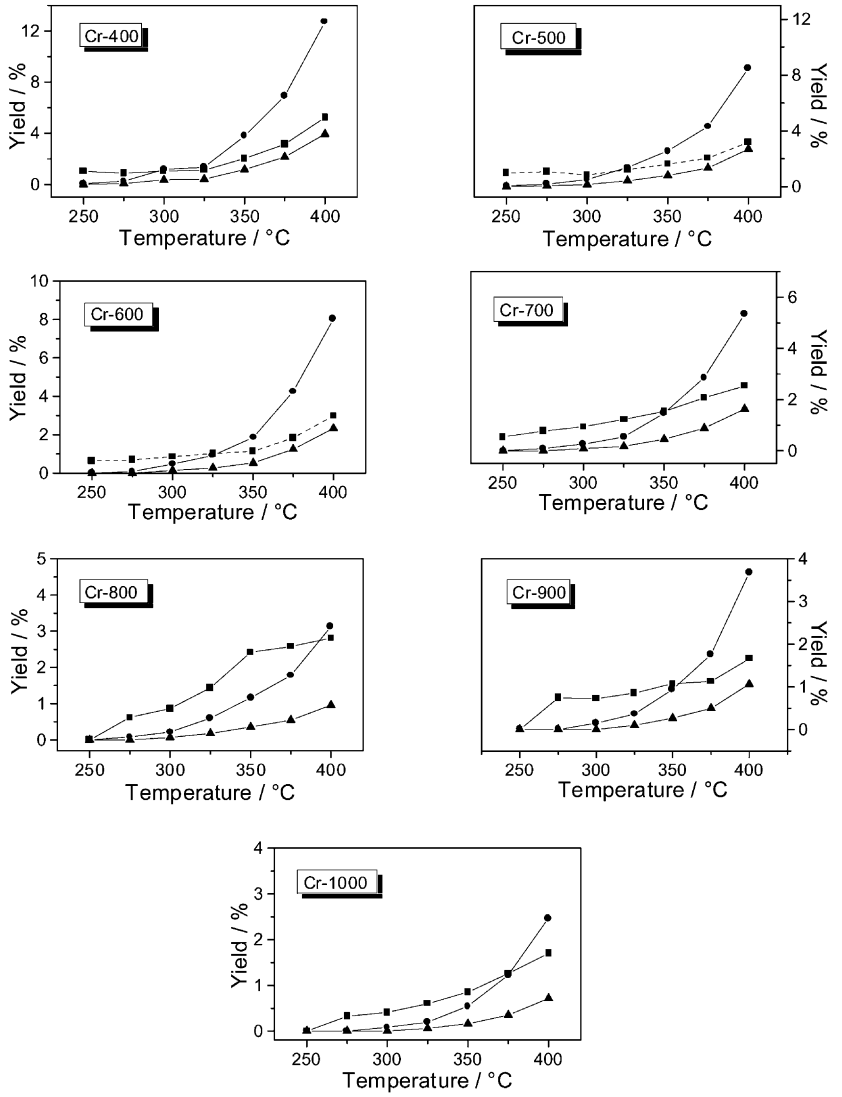

Fig. 3. Variation of the yield percentage of acetaldehyde (■), ethylene (●), and ethane (▲) as a function of the reaction temperature for the calcined chromia catalysts.

4. The fourth possibility consists of the secondary hydrogenation of ethylene by hydrogen (dehydrogenation by product), as it was claimed by the early investigations of McMonagel and Moffat [25] for ethane production by ethanol decomposition over 12-molybdophosphates:

$$C_2H_5OH \rightarrow C_2H_4 + H_2O \quad (4)$$

$$C_2H_4 + H_2 \rightarrow C_2H_6 \uparrow \quad (5)$$

Thus, this literature survey leaves the interesting question: to which of the forgoing pathways does ethane formation over Cr-*x* and Cd/Cr-*x* catalysts belong. Preliminary, the catalysts screening revealed the lack of observation of diethyl ether during ethanol decomposition all over the tested reaction temperatures (150–400°C). Hence, one can reasonably neglect the first two routes, since ethane formation throughout these two routes is essentially related to the presence of ether molecules. In order to judge which of the

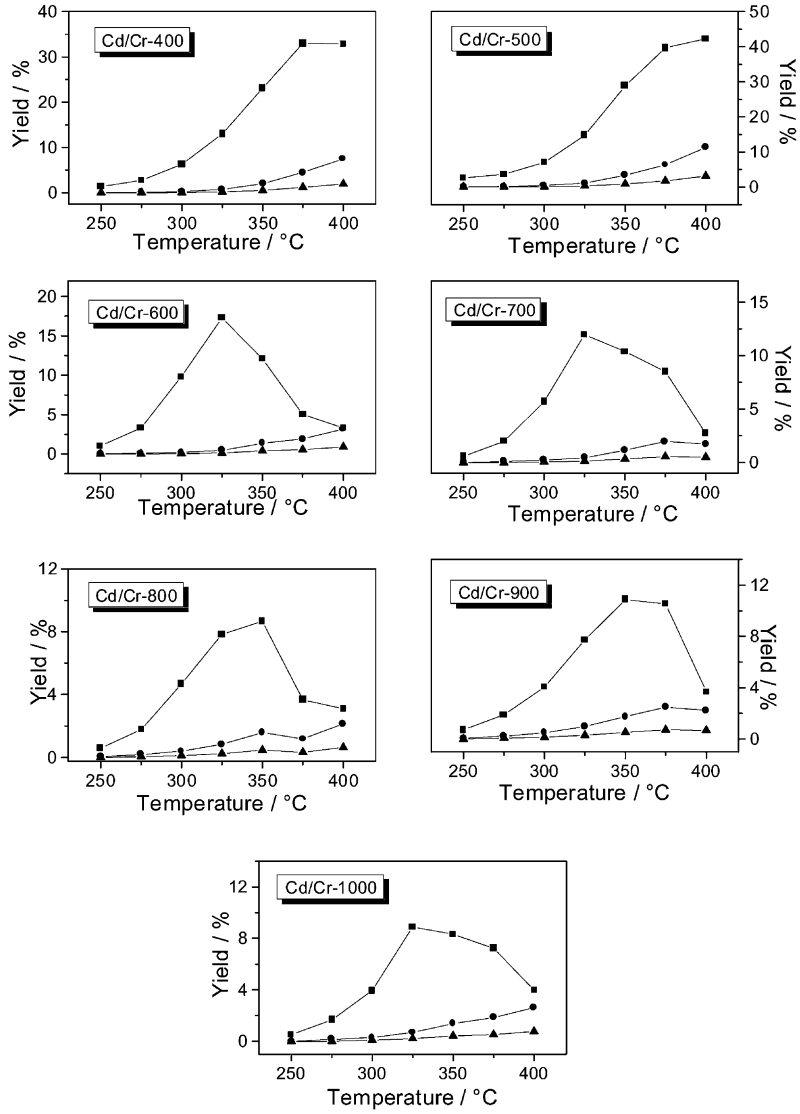

Fig. 4. Variation of the yield percentage of acetaldehyde (■), ethylene (●), and ethane (▲) as a function of the reaction temperature for the calcined cadmium/chromia catalysts.

other two pathways controls ethane production, in our case, we plotted both the ethylene and acetaldehyde selectivities against the ethane selectivity. Fig. 6 shows the obtained results over the 400–700°C calcined catalysts in both series. An inspection of these X-shaped relations revealed the existence of a linearity (with correlation coefficients higher than 0.999) between the hydrocarbons selectivities. On the other hand, an inverse relationship between ethane and acetaldehyde selectivities is evident. In the recent literature reports, about the hydride formation on chromia and transition metal chromites, there are some important contributions. Busca [45] demonstrated, based on H (D) isotopic shift and on a comparison with the spectra of known hydride species that terminal hydrides, Cr–H, are formed on chromia, whereas on some transition metal chromites, both terminal and bridged species, thought to be bounded to Zn^{2+}, Co^{2+}, and Mn^{2+}

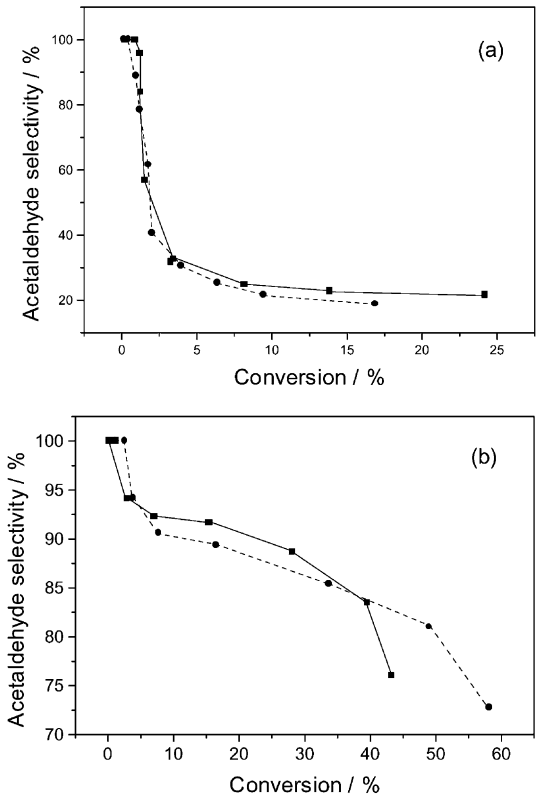

Fig. 5. Variation of acetaldehyde selectivity percentage as a function of the conversion percentage for the 400°C (■) and 500°C (●) calcined catalysts in chromia (a) and cadmium/chromia (b) catalysts.

centers, are observed. These transition metal hydrides were identified as the active species in hydrogenation over chromia [46] and on copper chromite [47] catalysts. Thus, from the parallelism between the experimental results and the literature data, we may assign the fourth route, secondary hydrogenation, to describe ethane formation over the catalysts under investigation.

Concerning the activity of chromia catalysts, many authors [44,48] relate the alcohol conversion activity (dehydration/dehydrogenation) over Cr_2O_3 catalyst to the presence of Cr^{6+}–Cr^{3+} Zener phase [49]. In this sense, we tried to determine the concentration of the water-extractable Cr^{6+} ions after the Cr-*x* catalysts have been used, but our results showed the absence of such ions. The disappearance of Cr^{6+} ions can be reasonably related to the $Cr^{6+} \rightarrow Cr^{3+}$ reduction process occurred during the catalyst usage. Accordingly, the activity of Cr-*x* catalysts cannot be related to the so-called surface mobile-electron Zener phase [49]. Knowing that an alcohol molecule can be hydrogen-bounded to an oxide through OH^- and O^{2-} groups of its surface [50]. Burwell et al. [51], using the theory of coordinative chemisorption [52], have stressed the important effect of water bound to the surface of chromium oxide in the form of hydroxyl groups. With regard to the dehydration reaction, many investigators [5,9,16,17,25,50] have considered the active sites for this reaction are of acidic character, i.e. Brönsted and Lewis sites. For Cr-*x* catalysts, increasing the pretreatment temperature leads to dehydration of the catalyst, which in turn increases the polarization of Cr–OH bond. As a result, an increase in the acidic strength of residual OH groups occurred. This process is maximized for the 400°C calcined catalyst, a sample that showed the highest dehydration activity in the Cr-*x* series. A similar interpretation was given also for the dehydration of isopropanol over ceria [50]. In accordance, it was reported [53] that the most active phase of chromium oxide is that persistent at 400°C calcination temperature, which contained the greatest extent of OH groups acting as active sites for isopropanol dehydration.

The Cr^{3+} ions are thought to be present in octahedral coordination in stoichiometric spinels, they are also present in the same coordination in Cr_2O_3 which, however, has the corundum structure [54]. Moreover, it was established from the crystal field consideration that $3d^3$:Cr^{3+} gains maximum ligand field stabilization energy (LFSE) from the octahedral geometry [55]. Therefore, the incompletely coordinated Cr^{3+} ions in the surface planes will have much stronger tendency to complete six-fold coordination [56]. Thus, these coordinatively unsaturated octahedral Cr^{3+} sites were considered as suitable adsorption sites for 2-propanol [17] via the unpaired electrons of their hydroxyl groups and CO [54] which involves electron donation towards the bands of the solid [57]. Treating the chromia catalysts at higher temperatures is expected to increase the dehydration of the catalyst, according to $2OH^- \rightarrow H_2O + O^{2-}$, which is accompanied by an increase in the number of coordinatively unsaturated Cr^{3+} ions (Lewis acid sites) on the catalyst surface. In a conclusion, by loss of water from the samples calcined at temperatures higher than 400°C,

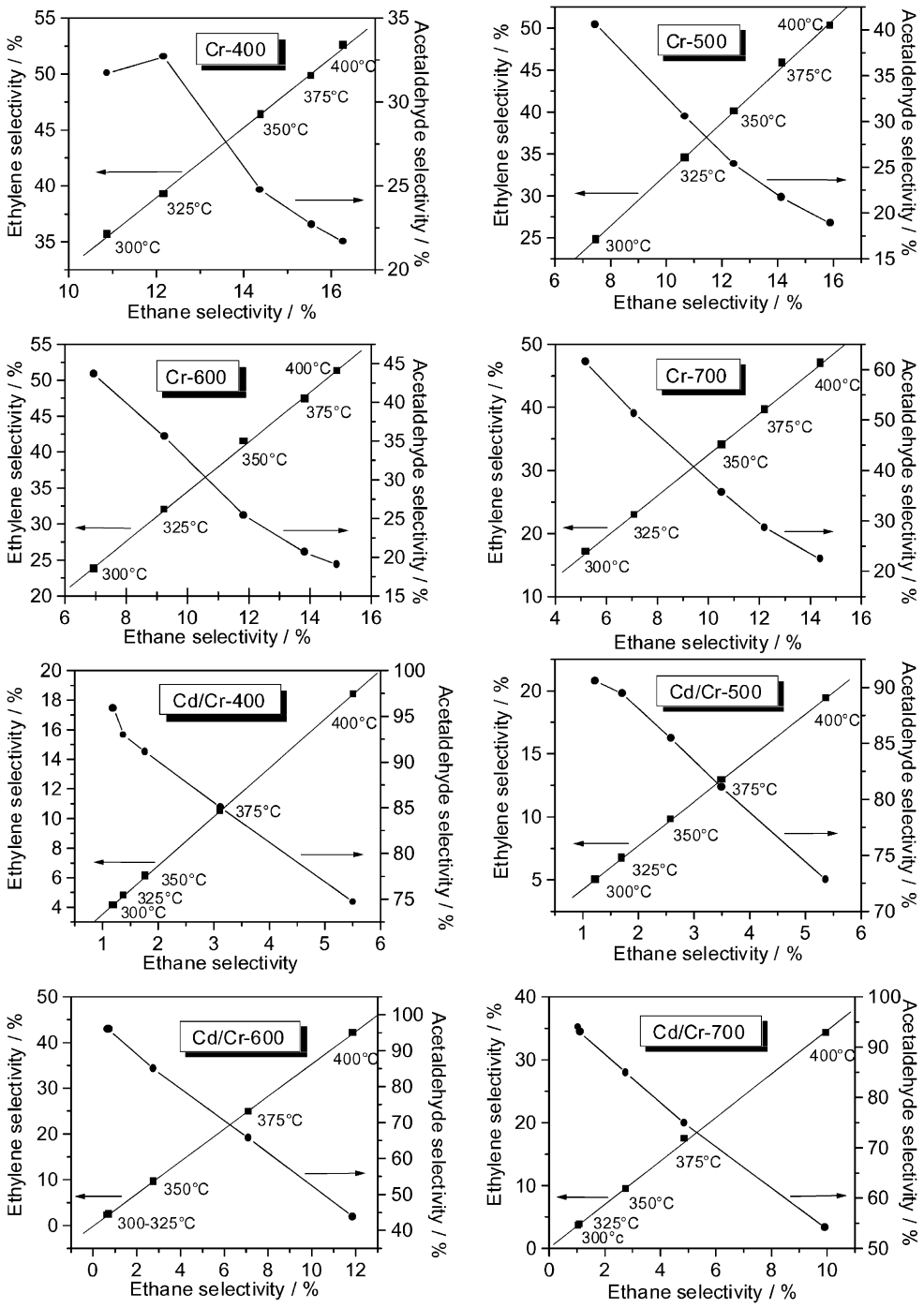

Fig. 6. Variation of ethylene as well as acetaldehyde selectivities with ethane selectivity in the 300–400°C reaction temperature range over the 400–700°C calcined catalysts in both series.

coordinatively unsaturated Cr^{3+} and O^{2-} are formed which constitute together the active centers for dehydration on chromia catalysts. Hence, the dehydration activity of Cr-*x* series is related to the presence of Brönsted and/or Lewis acid sites.

Considering the dehydrogenation activity of chromia, chromium oxide is known to be p-type semiconductor [44]. Moreover, it has been suggested [58] that p-type semiconductor is better dehydrogenating catalyst than n-type semiconductor. Furthermore, correlating the electronic reflectance spectra of a series of chromium oxide preparations with their catalytic activity revealed that the dehydrogenation of alcohols proceed on the surface of Cr^{3+} [59]. Consequently and in agreement with our recent work on silver-chromia catalysts [2], it is plausible to suggest that acetaldehyde is formed on Cr^{3+} sites.

Following up the variation of the conversion percentage as well as the products yield with the calcination temperature, two points could be raised in this respect: (i) the lower dehydrogenation yield, compared to the dehydration one, is a direct response to the effect of water (dehydration by product) which is known to inhibit alcohols dehydrogenation over chromia catalysts [44]; (ii) the decrease in the conversion percentage upon raising the calcination temperature matches beautifully with the increase in the activation energy of conductance (cf. Fig. 10 in part I of this work) as well as the decrease in the catalysts surface areas due to the progress of the sintering process (cf. Table 3 in part I of this work). If one assume that two-point adsorption of alcohols are necessary for the dehydration activity and that can take place most readily in the pores [60]. One may arrive at the conclusion that on a sintered catalysts, there are few pores and the two-point desorption is less feasible. Consequently, a decrease in the activity is expected.

Under the light of the previous discussion, it is plausible to relate the dehydration and the dehydrogenation activities of Cr-*x* catalysts to the surface-exposed ions, viz. coordinatively unsaturated Cr^{3+}, O^{2-}, and/or OH^-. Thus, the suggested reaction mechanism for ethanol decomposition over group IVB oxides [5] can be employed here. In this mechanism, ethylene as well as acetaldehyde are produced throughout an alkoxide intermediate, which in turn is formed via the reaction of ethanol with surface OH^- or O^{2-} groups. Ethylene is formed by the β-H elimination from alkoxide, which involves H-donation to Cr^{3+} cation, followed by its rapid transfer to the oxygen atom during the breaking of C–O bond. On the other hand, acetaldehyde is produced through an α-H elimination from alkoxide intermediate.

It is of interest to note that by comparing the Cr-*x* and Cd/Cr-*x* series, the higher activity of the latter (especially for Cd/Cr-400 and Cd/Cr-500 catalysts) cannot be explained in terms of surface area variations, since Cr-*x* catalysts were proved to have a higher S_{BET} values (cf. Table 3 in part I of this work). Moreover, we measured the surface areas for the used Cd/Cr-*x* catalysts. The results are cited in Table 1. Inspection of this table revealed, in general, that there is no marked difference in S_{BET} values between the fresh and the used catalysts. As a result, one may state that the change in the activity of the Cd/Cr-*x* catalysts cannot be explained in terms of surface area changes. In this regard, estimation of water-extractable Cr^{6+} ions for the used Cd/Cr-*x* catalysts showed the disappearance of such ions (Table 1), which directly responds to the $Cr^{6+} \rightarrow Cr^{3+}$ transformation. This bears out

Table 1
Surface area and water-extractable Cr^{6+} concentrations for the fresh as well as the used Cd/Cr-*x* catalysts

Calcination temperature (°C)	Fresh catalysts		Used catalysts	
	S_{BET} ($m^2\,g^{-1}$)	$Cr^{6+} \times 10^{-4}$ ($mol\,g^{-1}$)	S_{BET} ($m^2\,g^{-1}$)	$Cr^{6+} \times 10^{-4}$ ($mol\,g^{-1}$)
400	5.77	126.6	5.86	–
500	6.1	147.9	5.39	–
600	4.49	0.69	4.16	–
700	4.27	0.67	4.9	–
800	4.55	0.57	5.48	–
900	4.03	0.57	4.49	–
1000	2.8	0.3	3.1	–

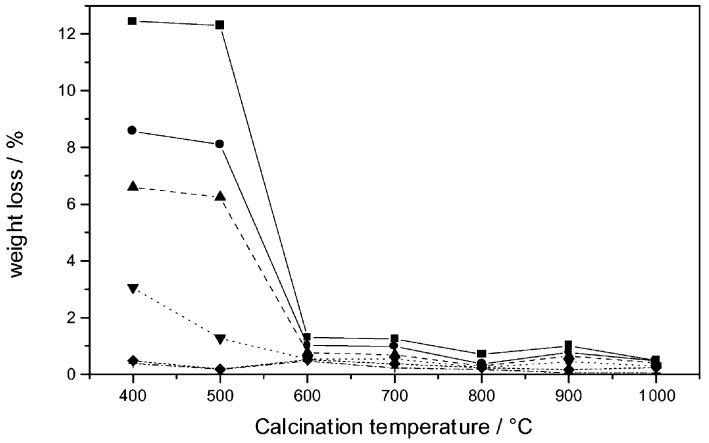

Fig. 7. Variation of the weight loss percentage (as obtained from isothermal EtOH-TPR experiments) as a function of the calcination temperature at: 200°C (◆); 250°C (▼); 300°C (▲); 350°C (●); 400°C (■).

the idea that the activity of this series of catalysts is structure-dependent.

The very marked difference in activity and selectivity between the 400–500°C calcined catalysts on one hand and the 600–1000°C calcined ones on the other hand (Figs. 2 and 4), even though both contained the same stoichiometric amounts of cadmium and chromium ions, emphasizes and highlights the importance of in situ EtOH-TPR experiments. In this way, Cubeiro and Fierro [61], using Pd/ZnO catalysts and based on the H_2-TPR experiments, showed that hydrogen consumption at high temperatures (above 800 K) is associated with the reduction of bulk ZnO. Bearing in mind the fact that many chromates are reducible in hydrogen atmosphere [2,62] together with the ability of CdO to be reduced (vide infra), the in situ EtOH-TPR experiments were carried out for the cadmium-containing catalysts. The results are shown in Fig. 7 as weight loss percentage against the calcination temperature of Cd/Cr-*x* system. The measurements were carried out isothermally, 30 min for each reduction temperature. Two regions can be distinguished: (i) the first one belongs to 400 and 500°C calcination products; (ii) the second one belongs to the catalysts calcined at temperatures higher than 600°C. Generally, the change in the weight loss percentage of the second region upon raising the reduction temperature is very low (<1.5%), which reflects the refractory nature of cadmium chromite spinel towards reduction. Moreover, the maximum weight loss percentage observed for the 400 and 500°C catalysts, 12.45 and 12.31 under the catalytic conditions, respectively, is very close to that (13.1) expected for the bulk reduction of these two catalysts (both composed of $CdCrO_4 + (1/2)Cr_2O_3$ as shown previously in part I of this work) to yield $Cd^0 + Cr_2O_3$ mixture. In this context, it is worth mentioning that we observed a condensation of water at the cool-end of the TGA quartz tube. This suggests the following pathway:

$$(CdCrO_4 + \tfrac{1}{2}Cr_2O_3)_{\text{catal.}} + \tfrac{5}{2}H_{2_{\text{ethanol dehydrogenation}}} \rightarrow Cd^0 + Cr_2O_3 + \tfrac{5}{2}H_2O \quad (6)$$

The extent of cadmium chromate reduction would presumably depend upon the length of the time that the catalyst was exposed to the flow of the alcohol.

Reducibility of Cd/Cr mixture also finds another support from the FT-IR measurements. FT-IR spectra in the region 1200–400 cm^{-1} of the different Cd/Cr-*x* catalysts, taken from the reactor at the end of the catalytic run, are shown in Fig. 8. A close inspection of Fig. 8 reveals that the spectra of the tested Cd/Cr-400 and Cd/Cr-500 catalysts showed the disappearance of the bands characterizing the chromate ion vibrations, i.e. at 930–780 cm^{-1} [2,62–66], and the development of new bands at 629, 581, and 414 cm^{-1} which were assigned to Cr_2O_3 [2,65–67]. In this context, the presence of Cr_2O_3 as the only phase detected

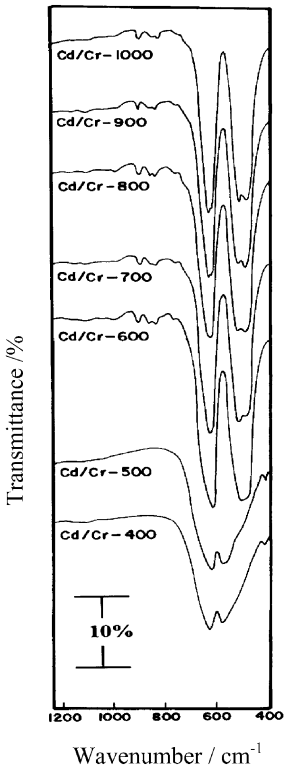

Fig. 8. FT-IR spectra obtained for the tested Cd/Cr-400, Cd/Cr-500, Cd/Cr-600, Cd/Cr-700, Cd/Cr-800, Cd/Cr-900, and Cd/Cr-1000 catalysts.

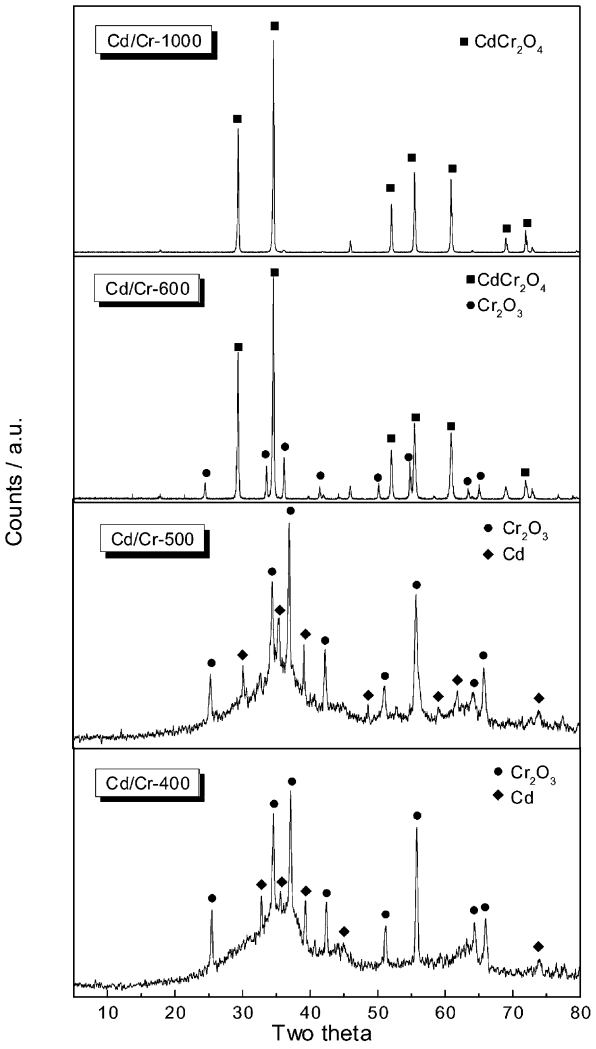

Fig. 9. XRD patterns recorded for the Cd/Cr-400, Cd/Cr-500, Cd/Cr-600, and Cd/Cr-1000 catalysts taken from the reactor at the end of the catalytic runs.

by FT-IR suggests that Cr^{6+} reduction under the used catalytic conditions is terminated by Cr^{3+} formation. Haber [68] pointed out that the removal of oxygen ion could be replenished in two ways: gaseous oxygen adsorbed on the vacancy sites, and the bulk lattice oxygen diffusion to the surface and entering the oxygen vacancy sites. In our case, lattice oxygen diffusion is high, since the measurements were done in the absence of oxygen, thus leading to bulk reduction. The FT-IR spectra of the 600–1000°C calcined catalysts, on the other hand, showed the same spectra reported in part I of this work [42], a fact which reveals the persistence of the cadmium chromite after activity measurements.

The phase changes accompanying the activity measurements of Cd/Cr-*x* catalysts were also checked by using XRD analysis. Fig. 9 reports the X-ray diffractograms of four used catalysts, Cd/Cr-400, Cd/Cr-500, Cd/Cr-600, and Cd/Cr-1000. In agreement with the results discussed in the preceding paragraphs, the tested Cd/Cr-400, and Cd/Cr-500 catalysts consist of a mixture of Cd^0 (with *d* at 2.34, 2.81, and 2.58 Å) and Cr_2O_3 (with *d* at 2.48, 2.67, and 1.67 Å) [69], whereas the other two catalysts showed reflections of $CdCr_2O_4$ as a major phase (with *d* at 2.60, 1.66, and 1.52 Å) [69]. Hence, the occurrence of reduced cadmium upon exposure to ethanol vapor is characteristic only for the samples composed of $CdCrO_4$ as a major phase, i.e. Cd/Cr-400 and Cd/Cr-500 ones. Reviewing

the literature revealed the presence of interesting examples considering the catalysts reducibility. More recently, it was shown [70] that reducing α-Fe_2O_3 with CO produces iron carbide, the latter showed higher ability and activity towards the conversion of primary and secondary alcohols than the former. The same authors, using XRD analysis, suggested that the higher activity of iron carbide catalyst implies that either the surface is not oxidized to the oxide during the conversion of alcohol or the oxycarbide that is formed on the iron carbide surface is more active than the iron carbide surface. Additional examples showed that when the coinage cations are mixed with chromia, reduction of these cations occurs leading to the formation of zerovalent metals supported on chromia. In this respect, Múèka [71] reported, for CuO–Cr_2O_3 system, that reduction of CuO with hydrogen was significantly affected by varying the percentage of Cr_2O_3 in the catalyst composition. In our laboratory, we did some experiments to assess the reducibility of Ag_2O–Cr_2O_3 mixture [2]. Our results showed that formation of Ag^0–Cr_2O_3 mixture is responsible for the high activity of this series of catalysts towards ethanol conversion.

With regard to the present results, it is really interesting to analyze why cadmium chromate rather than cadmium chromite is reduced. The answer of this question lies in two factors. First, cadmium chromite is essentially normal spinel, AB_2O_4, with the octahedrally coordinated cation position occupied exclusively by the trivalent cations [62]. The stoichiometric compound has the structural formula $(Cd^{2+})_{tet.}(Cr^{3+}Cr^{3+})_{oct.}O_4{}^{2-}$. Thus, in $CdCr_2O_4$, as with $ZnCr_2O_4$ [17,72], the surface-exposed ions are exclusively Cr^{3+} and O^{2-}, whereas the Cd^{2+} ions lie under the first surface layer with a complete tetrahedral coordination. Regarding the structure of $CdCrO_4$, Cr(VI) ions exist in a tetrahedral coordination with oxygen [73]. Thus, this structure gives a chance of cadmium ions to be exposed to the surface. In a conclusion, one factor responsible for the irreducibility of cadmium chromite catalyst, rather than chromate one, comes from the location of Cr^{3+} and O^{2-} on the crystal surface provides some sort of shielding of cadmium ions, consequently preventing them from being in contact with the attacking hydrogen molecules. The second factor comes from the reducibility of chromate ion itself. Inspection of the electrochemical series [74] demonstrated that, in solution, chromate ions are much easier to be reduced than chromite ones. Cadmium ions lie in between, but with a reduction potential closer to that of chromate ions. Such fact will be discussed later using TPR technique. Consequently, one can write the following scheme describing the reduction of cadmium chromate:

$$2CdCrO_4 + 3H_2 \rightarrow 2CdO + Cr_2O_3 + 3H_2O \quad (7)$$

$$CdO + H_2 \rightarrow Cd^0 + H_2O \quad (8)$$

From the forgoing discussion, it appears that the ability of catalysts containing cadmium chromate as a major phase, i.e. Cd/Cr-400 and Cd/Cr-500 catalysts, to be reduced in comparison with the refractory chromite one is the key factor controlling their catalytic activity behavior. Reduction of cadmium chromate, with hydrogen generated in situ, produces zerovalent cadmium supported on chromia which is accompanied by an evolution of the lattice oxygen. Accordingly, acetaldehyde formation on these surfaces can be realized as an oxidative dehydrogenation reaction. Moreover, the high dehydrogenation selectivity of these two catalysts, in comparison with the Cr-*x* as well as the rest of Cd/Cr-*x* catalysts, suggests that acetaldehyde is produced essentially over zerovalent cadmium (vide infra). Similar interpretation was employed in case of ethanol dehydrogenation over copper supported on Cr/Al [14] and on SiO_2, ZrO_2, and Al_2O_3 [9], where zerovalent copper atoms consist the active dehydrogenation centers.

Considering the activity of Cd/Cr-400 and Cd/Cr-500 catalysts, it is worth mentioning that the latter catalyst is more active than the former one, however both catalysts were proved to be composed of Cd^0–Cr_2O_3 mixture. This fact cannot be understood in terms of surface area differences, since both catalysts showed very similar S_{BET} values before and after reduction. Therefore, in order to find a valid interpretation for such variation, we calculated Cd^0 and Cr_2O_3 grain size in both catalysts base on XRD line width broadening and applying the Scherrer equation [75]. Data processing (including background correction, $K\alpha_2$ stripping, peak identification, and particle size analysis) was accomplished using the Traces (diffraction technology) software package. The average

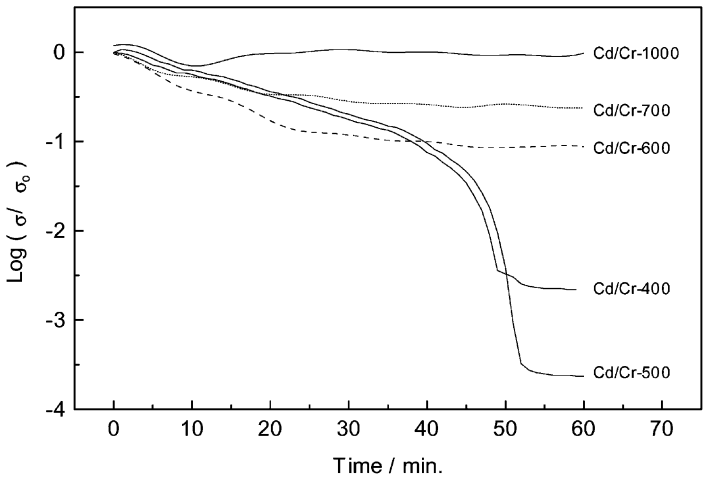

Fig. 10. Variation of the electrical conductivity ($\log \sigma/\sigma_0$) values with time after ethanol admission at 300°C for Cd/Cr-*x* catalysts.

particle size estimation for Cd^0 was 49.47 and 64.64 nm for Cd/Cr-400 and Cd/Cr-500 catalysts, respectively. In addition, the respective particle size for Cr_2O_3 was found to be 40.83 and 52.7 nm. From these values, it is evident that the constituents of the reduced Cd/Cr-500 catalyst have higher particle size than those of the Cd/Cr-400 ones. Two points could be referred to in this respect: (i) reduction of β-$CdCrO_4$ (major phase for the 500°C calcined catalyst) proceeds with the formation of Cd^0 as well as Cr_2O_3 having a larger particle size compared to those obtained by the reduction of α-$CdCrO_4$ (major phase for the 400°C calcined catalyst); (ii) the calculated particle size values could be considered as a reasonable factor for the higher activity of the 500°C calcined catalysts compared to the 400°C calcined one. At this point, Tsybulya et al. [76] examined a similar phenomenon concerning ethylene epoxidation over Ag/Al_2O_3 catalysts. These authors observed an activity increase as a result of increasing silver particle size. Moreover, Bhat et al. [77], working on the toluene alkylation on a series of ZSM-5 preparations, showed that zeolite batches containing longer crystals of oblong shape favored the *para*-isomer selectivity.

A primary goal of the present investigation was to measure changes in the electrical conductivity of the cadmium-containing catalysts resulting from adsorption and surface reaction process of ethanol. The results of in situ electrical conductivity measurements, upon admission of ethanol vapor at 300°C, are represented in Fig. 10 as $\log \sigma/\sigma_0$ versus time for the 400–700 and 1000°C calcined catalysts. The measurements were carried out at 300°C. Moreover, the conductivities obtained at the steady state after the admission of ethanol vapor to the Cd/Cr-*x* catalyst at 300°C are listed in Table 2. In contrast to the 600–1000°C calcined catalysts, 400 and 500°C ones exhibited a continuous decrease after about 40 min of alcohol admission. Then constant values are obtained. Meanwhile, these two catalysts manifest the highest conductivity values after alcohol admission (Table 2). As a result, the high initial conductivities of these two catalysts can be attributed, as shown in part I, to the coexistence of Cr(VI) and Cr(III)

Table 2
Electrical conductivities for the Cd/Cr-*x* catalysts after the admission of ethanol at 300°C

Calcination temperature (°C)	$\sigma \times 10^{-8}$ (Ω^{-1} cm^{-1})
400	18.52
500	27.78
600	5.41
700	2.94
800	1.26
900	1.49
1000	0.27

ions in the form of $CdCrO_4$ and Cr_2O_3, respectively, forming a stable mobile-electron Zener phase [49]. Ellison and Sing [78] reported that the presence of closely coupled Cr^{6+} and Cr^{3+} at the surface would facilitate the Zener mechanism, thus leading to the maximization of the conductivity. The break in electrical conductivity of $CdCrO_4$-containing catalysts in the presence of alcohol vapor indicates that a second type of charge carriers, other than those responsible for the oxidized catalyst, are in abundance at this point, viz. Cd^0–Cr_2O_3 couple.

Considering the Cd^0–Cr_2O_3 mixture, the formed zerovalent cadmium can be ionized thermally [79], giving interstitial Cd^{2+} ions and free electrons according to

$$Cd \rightleftharpoons Cd^+ + e^- \quad (9)$$

$$Cd^+ \rightleftharpoons Cd^{2+} + e^- \quad (10)$$

This process may facilitate a hopping conduction with electrons jumping from one cadmium site (Cd^0) to another (Cd^+ or Cd^{2+}). On the other hand, it has been shown that [44] the semiconducting properties of chromia catalysts suffer a p- to n-type transition on either heating the catalyst in alcohol atmosphere or doping with Cd^{2+} or Ce^{4+} ions. Therefore, one may arrive at the conclusion that reduction of cadmium chromate proceeds with formation of materials having new conductivity properties, probably n-type semiconductors, viz. Cd^0 and Cr_2O_3, which are responsible for the higher conductivity values of Cd/Cr-400 and Cd/Cr-500 catalysts after ethanol admission (Table 2) compared with the other catalysts in this series. Concurrent with this, the absence of the break in electrical conductivity of the 600–1000°C calcined catalysts can be easily understood taking into account the fact that these samples composed mainly of cadmium chromite spinel which is irreducible under our experimental conditions.

Recalling our activity results of this system (Figs. 2 and 4), one can observe a clear parallelism between the decrease in the activity as well as the in situ conductivity values as a result of raising the calcination temperature. This provides a support for the concept that the catalytic reaction is controlled by electronic functions, where the ease with which an electron can be transported from the bulk seems to be of great importance in determining the extent of adsorption process. Hence, the activity and selectivity of the 600–1000°C catalysts can be explained on the basis of the progress in the spinel phase formation with increasing the temperature as well as the coordination and electronic state of the cations exposed in the surface planes of the spinel, which contain coordinatively unsaturated B-site cations [17,71,80]. These sites will seek to neutralize the excess positive charge by electron movement either by adsorption from a negatively bound entity or by electron movement from the bulk of the solid [80]. Since, electron movement from the bulk of the solid will become significant only when each Cr ion has at least one Cr nearest neighbor [81], in the 600–1000°C calcined catalysts, the Cr ion sites will be electronically isolated (such effect will increase by increasing the calcination temperature up to 1000°C as shown by increasing the activation energy of conductance, cf. Fig. 10 in part I of this work). Thus, neutralization of such sites will not likely be by electron transfer, but by trapping electrons from the oxygen end of ethanol molecules. In this respect, it is reported [82] that the adsorption of an alcohol molecule by means of free electron pair of its oxygen atom on an electron-deficient center leads to dehydration. Acetaldehyde production on $CdCr_2O_4$ surfaces can be related, as shown with Cr-*x* catalysts, to the presence of surface coordinatively unsaturated Cr^{3+} cations, since Cd^{2+} ions lie under the first surface layer.

The higher dehydration and dehydrogenation yields over Cd^0–Cr_2O_3 mixture can be easily understood as follows. Upon alcohol dehydration, water desorption is favored by a surface having high electron concentration [17]. In addition, desorption of water seems to be the most likely rate-determining step [83]. It follows that the dehydration selectivity is improved by the increase of the surface electron concentration. The latter is higher the higher Cd^0 concentration, i.e. the higher the sample electrical conductivity. Inspection of the conductivity data (Table 2) shows that after alcohol admission, the electrical conductivities of Cd/Cr-400 and Cd/Cr-500 catalysts are 18.52×10^{-8} and $27.78 \times 10^{-8}\ \Omega^{-1}\,cm^{-1}$, respectively, are higher than those of the rest of the catalysts in this series. Consequently, higher dehydration yield is observed. Regarding the high dehydrogenation activity of Cd^0–Cr_2O_3, it was shown [84] that changes in conductivity accompanying the dehydrogenation of ethanol, at temperatures >

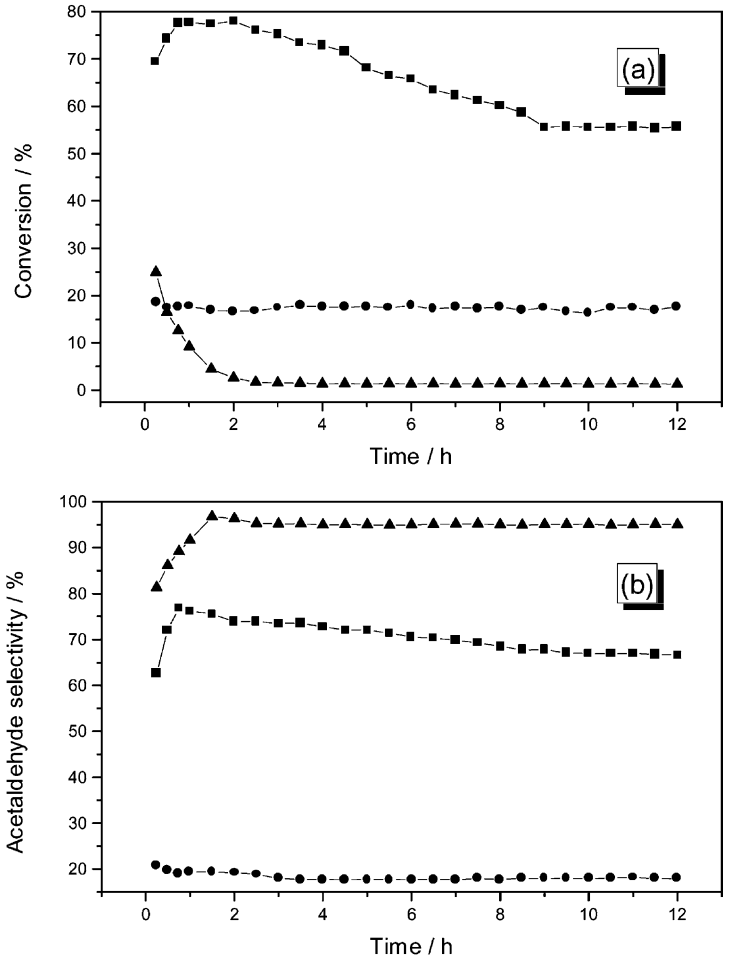

Fig. 11. Effect of time on the conversion percentage (a) as well as the acetaldehyde selectivity (b) over Cd-500 (▲), Cr-500 (●), and Cd/Cr-500 (■) catalysts.

225°C over ZnO, indicate net donor adsorption. These authors [84] suggested, in view of the strong acceptor behavior of acetaldehyde that this product desorbed immediately upon formation. In conclusion, it seems probable that the donating nature of Cd^0–Cr_2O_3 mixture provides a suitable environment for acetaldehyde production over such surfaces.

In view of the present results, it could be assumed that high dehydrogenation activity required the simultaneous presence of Cd^0–Cr_2O_3 pair. Accordingly, it is really interesting to do further analysis in order to visualize the effect of incorporation of CdO and Cr_2O_3 on the high activity of cadmium/chromia mixture. In this regard, we prepared a sample of CdO (denoted Cd-500) via the thermal decomposition of cadmium carbonate and tested its activity towards ethanol decomposition. Fig. 11a gives the effect of time on ethanol conversion over Cd-500, Cr-500, and Cd/Cr-500 catalysts. The measurements were done under the same conditions mentioned earlier and at 400°C reaction temperature. Inspection of Fig. 11a revealed that the activity of Cd/Cr catalyst first increases, goes through a maximum, then declines slowly reaching a steady state after 9 h. The increase in the activity observed during the beginning of the measurements is due to the presence of Cr^{6+} ions on

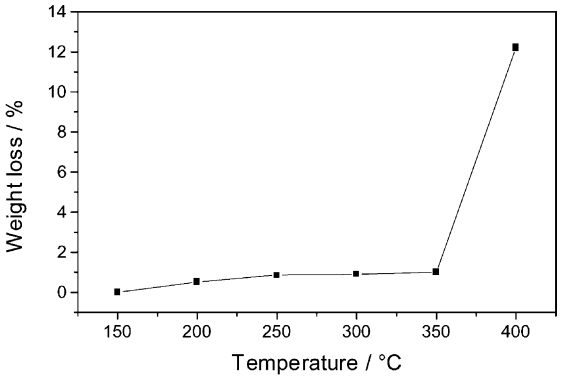

Fig. 12. Variation of the weight loss percentage (as obtained from isothermal EtOH-TPR experiments) at elevated temperatures for CdO catalysts.

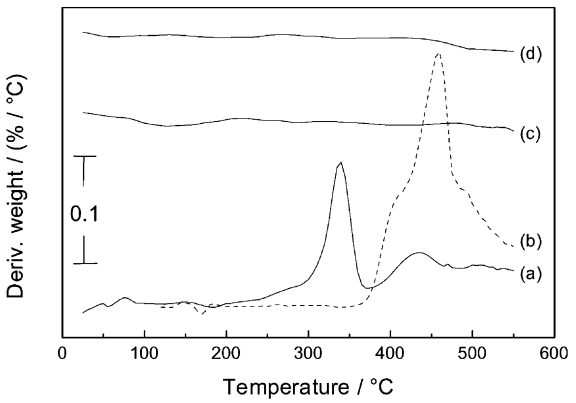

Fig. 13. TPR curves (as obtained from non-isothermal experiments) for the catalysts: Cd/Cr-500 (a); Cd-500 (b); Cr-500 (c); Cd/Cr-600 (d).

the surface of the catalyst. This is confirmed by the Cr^{6+} determination before the activity measurements (cf. Table 1). The decrease in the activity can be ascribed, as shown before, to the $CdCrO_4$ reduction process leading to the formation of Cd^0–Cr_2O_3 mixture. Meanwhile, Cr-500 catalyst shows a constant conversion percentage (about 19%) all over the time scale for the measurements. Cd-500 exhibits an initial activity of about 26% conversion, which decreased continuously in 2 h reaching about 2%, then stabilized. In this context, EtOH-TPR measurements for CdO (Fig. 12) disclosed that at 400°C, the oxide suffered a 12.22% weight loss which is very close to the value expected for Cd^0 formation (12.46%). Therefore, the decrease in the activity observed for Cd-500 sample can be undoubtedly related to $Cd^{2+} \rightarrow Cd^0$ reduction process.

From Fig. 11a, it is clear that Cd/Cr catalyst is significantly more active than both Cr and Cd ones, confirming the synergistic effect of Cd^0–Cr_2O_3 mixture. From the selectivity pattern (Fig. 11b), it is evident that Cd-500 catalyst shows a high dehydrogenation selectivity (about 95%), whereas Cr-500 one gives low dehydrogenation selectivity (about 19%). Meanwhile, Cd/Cr-500 catalyst manifests selectivity values displaced to higher values over the entire time scale. This trend suggests again that ethanol dehydrogenation occurs principally on Cd^0 sites, but is promoted in some manner by chromium centers. Let us consider the reducibility of these three catalysts.

Fig. 13 reports the EtOH-TPR results (the measurements were done non-isothermally by heating each sample in an alcohol atmosphere, 10°C min^{-1}, till 550°C) which are represented in the form of differential thermogravimetric (DTG) profiles for Cd/Cr-500, Cd-500, and Cr-500 catalysts (curves a–c, respectively). A DTG profile corresponding to a catalyst containing chromite phase (Cd/Cr-600 catalyst) is also included for comparison purpose (curve d). Four points can be extracted from these data in Fig. 13: (i) Cr_2O_3 catalyst (curve c) showed the absence of any weight change upon heating a fact which reflects its irreducibility under the used conditions; (ii) CdO catalyst (curve b) exhibits one peak maximized at 465°C which is accompanied by a total weight loss of 12.63%, a value that is in a good agreement with the calculated one for the Cd^0 formation (12.46%); (iii) $CdCrO_4$-containing catalyst shows two peaks being located at 342 and 438°C, which give rise to 7.56 and 12.42 weight loss percentage, respectively. Such values match satisfactorily with those corresponding to the formation of $CdO + Cr_2O_3$, and $Cd^0 + Cr_2O_3$, respectively, based on the starting material is composed of $CdCrO_4 + (1/2)Cr_2O_3$. This means that reduction of $CdCrO_4$ producing Cd^0–Cr_2O_3 mixture passes through CdO–Cr_2O_3 intermediate, which confirms the validity of the proposed reduction pathway given in Eqs. (7) and (8). Furthermore, the presence of chromium ions enhances the $Cd^{2+} \rightarrow Cd^0$ reduction process as shown by the shift of T_{max} due to

cadmium ions reduction from 465 to 438°C; (iv) the resistivity of $CdCr_2O_4$ spinel towards reduction can be inferred again from the absence of any reduction peak during the measurements (curve d). This is in line with the data obtained from the electrochemical series by confirming that chromate ions are easier to be reduced than cadmium ions, whereas chromite ones need higher potentials.

Many investigators have searched for an explanation of the synergic effect. Delmon and coworkers [85–88] proposed the remote control mechanism (RCM) to explain many experimental results concerning multiphase catalysts. According to this mechanism, a donor phase (a metal oxide) activates molecular oxygen and forms a mobile species which migrates to an acceptor phase (another oxide) to react with its surface and create or regenerate the sites which form selectively the partially oxygenated products. Other scientists relate the enhancing effect to an electronic factor. In this way, Harris and Chianelli [89] showed that the donation of electrons to Mo is responsible for promoting the hydrodesulfurization activity of Mo-based catalyst. A third opinion deals with the geometric effect, here a "short range" and "long range" interactions were used to describe the surface synergism between copper and its oxides towards isopropanol dehydrogenation [34].

According to the previously discussed experimental arguments, a possible interpretation of the Cd^0–Cr_2O_3 synergism in ethanol conversion might be that chromium enhances the activity of cadmium by promoting and stabilizing its reduction conditions (as shown by the non-isothermal EtOH-TPR measurements, Fig. 13). A similar interpretation was used to explain the enhanced activity of alumina-supported Pt/Rh bimetallic catalysts [90]. Another possible interpretation could be that the nearest neighbors to a given surface site may influence the adsorptive and hence the catalytic properties of another active site by forming together an "acceptor–donor" pair which provides a suitable environment for alcohol adsorption, then decomposition, i.e. an electronic effect. Accordingly, and taking into account the electrical conductivity results, Cd^0 can act as donor site, whereas surface coordinatively unsaturated Cr^{3+} can act as electron acceptor. Consequently, ethanol dehydration can be represented by the following scheme:

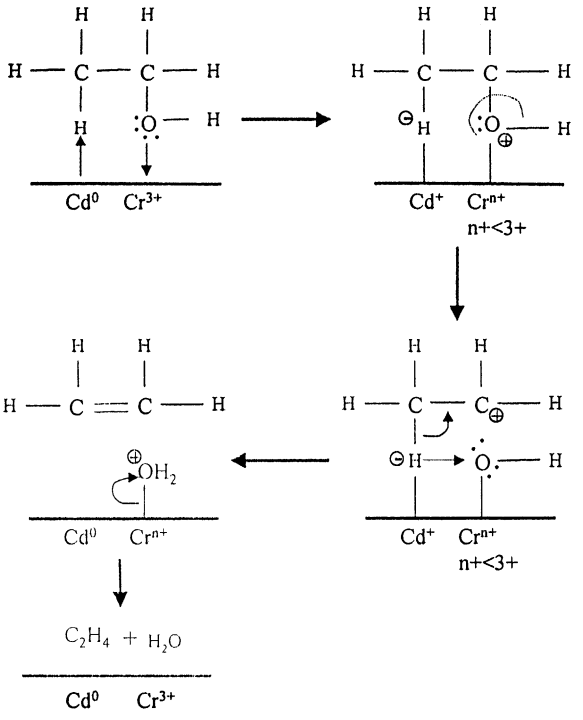

The dehydrogenation pathway can proceed as follows:

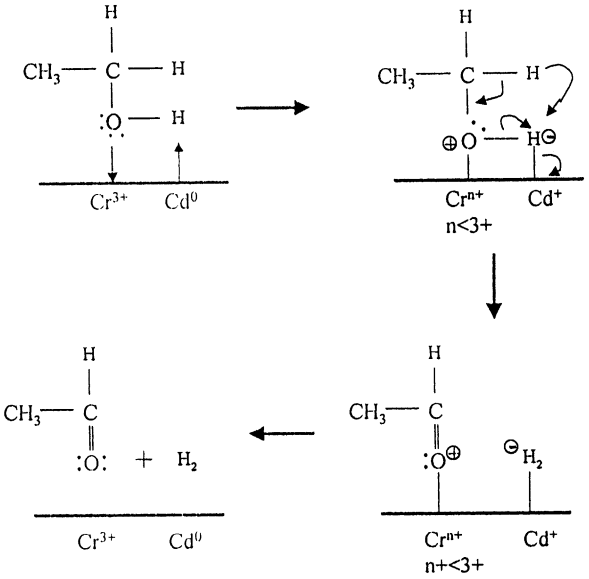

Since the 400 and 500°C calcined catalysts showed an interesting activity features. Hence, the study now will be devoted to shed some light on the effect of

changing the *W*/*F* and the activity of these catalysts. Moreover, kinetic studies of ethanol decomposition on the same catalysts will be concerned. The experimentally determined relationship between the conversion percentage and *W*/*F*, in the temperature range 275–400°C, is represented in Fig. 14a and b for Cd/Cr-400 and Cd/Cr-500 catalysts, respectively. The reciprocal space velocity (*W*/*F*) was changed by changing the weight of the catalyst charged into the reactor. It is evident that increasing *W*/*F* is accompanied by an increase in the conversion percentage, meanwhile Cd/Cr-500 catalyst is more active than Cd/Cr-400 one along the *W*/*F* range. Moreover, the dehydrogenation selectivity (not shown) of the two catalysts lie in the range 73–79% all over the tested *W*/*F* range.

Because of the conversion percentage over both catalysts increases smoothly with the temperature, it was used to estimate the rate constant (k) as well as the energy of activation (E_a), assuming that the reaction is of first order. The specific rate constants were calculated according to [91]

$$k = \frac{F}{W} \ln \frac{1}{1 - X}$$

where X is the degree of conversion, F the flow rate, and W the weight of the catalyst. The activation energies were calculated by applying Arrhenius equation, i.e. by plotting the $\ln k$ against the reciprocal absolute temperature. Table 3 summarized the values of the specific rate constant as well as the activation energy

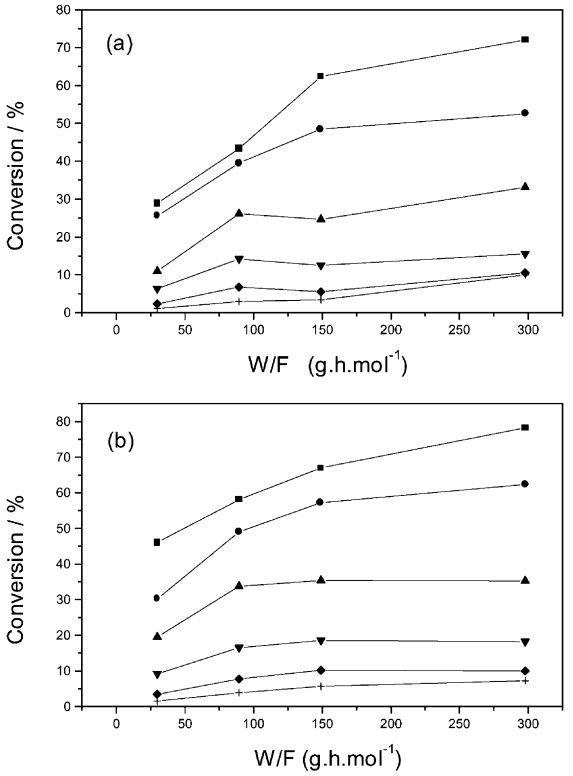

Fig. 14. Conversion of ethanol as a function of *W*/*F* for Cd/Cr-400 (a) and Cd/Cr-500 (b) catalysts. The measurements were carried out at 275°C (+), 300°C (◆), 325°C (▼), 350°C (▲), 375°C (●), and 400°C (■).

Table 3
Experimentally determined rate constant (k) and activation energy (E_a) values for ethanol decomposition over Cd/Cr-400 and Cd/Cr-500 catalysts between 300 and 400°C

$W/F \times 10^{-3}$ (kg h mol^{-1})	$k \times 10^{-2}$ (m^3 h^{-1} kg^{-1})					E_a (kcal mol^{-1})
	300°C	325°C	350°C	375°C	400°C	
Cd/Cr-400						
30	6.31	17.58	31.33	79.48	92.09	6.62
89	19.83	45.31	89.03	135.75	153.14	5.13
149	15.26	36.00	76.33	178.91	264.16	6.99
298	30.10	45.60	108.62	200.89	344.09	6.03
Cd/Cr-500						
30	3.47	25.91	58.71	97.08	166.62	8.84
89	21.73	48.7	111.16	181.64	234.68	5.87
149	29.07	55.45	118.08	229.39	299.09	5.83
298	28.357	54.29	139.73	263.39	411.4	6.63

values for Cd/Cr-400 and Cd/Cr-500 catalysts at different W/F values. Inspection of these values revealed that both catalysts exhibit similar activation energies of 5–9 kcal mol^{-1} between 300 and 400°C. This can be considered as another conformation of the structural identity of these two catalysts.

4. Conclusions

The information collected in the present study allows the following conclusions to be drawn.

1. Ethanol decomposition over Cr-*x* and Cd/Cr-*x* catalysts proceeds with the formation of ethylene, ethane, and acetaldehyde as the major products. Dehydrogenation selectivity was strongly dependent on both the reaction temperature and ethanol conversion. Cadmium-containing catalysts specially those calcined at 400 and 500°C showed higher dehydrogenation selectivity than Cr-*x* catalysts. Our suggested explanation of the alkane production implies that parallel hydrogenation and dehydrogenation reactions are necessary, with the dehydrogenation one producing the required hydrogen.
2. As to the dependence of the activity of Cd/Cr-*x* catalysts on their structural properties, our results showed that the samples containing chromate phase is more active than the catalysts containing chromite phase. With the aid of EtOH-TPR, XRD, and FT-IR analyses as well as the in situ electrical conductivity measurements, $CdCrO_4$-containing catalysts are reduced, via the hydrogen generated in situ. The extent of reduction would presumably depend on the length of time that the catalyst was exposed to the flow of alcohol as well as the temperature of the measurements. On the other hand, cadmium chromite spinel was irreducible. This could be attributed to structural and electronic properties of the spinel itself.
3. Ethanol decomposition over Cd/Cr-400 and Cd/Cr-500 catalysts is consistent with the autocatalytic process featuring: (i) an initial oxidative dehydrogenation process leading to nucleation and growth of Cd^0 particles on the Cr_2O_3; (ii) the progressive acceleration of the dehydrogenation activity as the number and size of Cd^0 metallic particles increased.
4. Thanks to the present results, we can demonstrate that the coexistence of Cd^0 and Cr_2O_3 as a result of $CdCrO_4$ reduction provides a synergistic enhancement of ethanol decomposition activity. The present work shows that Cr_2O_3 needs to be accompanied by a donor phase to achieve better performances. Thus, we suggest that Cd^0 in case of Cd^0–Cr_2O_3 mixture plays a role of donor.

References

[1] I. Wender, Catal. Rev. 26 (1984) 304.
[2] B.M. Abu-Zied, Appl. Catal. A 198 (2000) 139.
[3] S. Arsalane, M. Ziyad, G. Coudurier, J.C. Vèdrine, J. Catal. 159 (1996) 162.
[4] G.J. Miller, M.L. Nelson, P.J.R. Uwins, J. Catal. 169 (1997) 143.
[5] G.A.M. Hussein, N. Sheppard, M.I. Zaki, R.B. Fahim, J. Chem. Soc., Faraday Trans. 1 87 (1991) 2655–2661.
[6] M.A. Bañares, H. Hu, I.E. Wachs, J. Catal. 150 (1994) 407.
[7] W. Zhang, A. Desikan, S.T. Oyama, J. Phys. Chem. 99 (1995) 14468.
[8] J.S. Chung, R. Miranda, C.O. Bennett, J. Catal. 114 (1988) 398.
[9] N. Iwasa, N. Takezawa, Bull. Chem. Soc. Jpn. 64 (1991) 2619.
[10] V.K. Raizada, V.S. Tripathi, D. Lal, G.S. Singh, C.D. Dwivedi, A.K. Sen, J. Chem. Technol. Biotechnol. 56 (1993) 265.
[11] N.E. Quaranta, J. Soria, V.C. Corberán, J.L.G. Fierro, J. Catal. 171 (1997) 1.
[12] L. Briand, L. Gambaro, H. Thomas, J. Catal. 161 (1996) 839.
[13] A.M. El-Awad, E.A. Hassan, A.A. Said, K.M. Aba El-Salam, Monatshefte Chem. 120 (1989) 199.
[14] N. Kanoun, M.P. Astier, G.M. Pajonk, J. Mol. Catal. 79 (1993) 217.
[15] J.E. Rekoske, M.A. Bateau, J. Catal. 165 (1997) 57.
[16] M.J.L. Gines, E. Iglesia, J. Catal. 176 (1998) 155.
[17] R.M. Gabr, M.M. Girgis, A.M. El-Awad, B.M. Abu-Zied, Mater. Chem. Phys. 39 (1994) 53.
[18] M.M. Girgis, J. Mater. Sci. 29 (1994) 80.
[19] R.M. Gabr, A.M. El-Awad, M.M. Girgis, Mater. Chem. Phys. 30 (1991) 69.
[20] W.-H. Cheng, J. Catal. 158 (1996) 477.
[21] A.A. Said, Bull. Chem. Soc. Jpn. 65 (1992) 3450.
[22] R. Sumathi, K. Johnson, B. Viswanathan, T.K. Varadarajan, Appl. Catal. A 172 (1998) 15.
[23] R. Rudham, A.I. Spiers, J. Chem. Soc., Faraday Trans. 1 93 (1997) 1445.
[24] M. Derewiński, S. Dźwigaj, J. Haber, Zeolites 4 (1984) 214.
[25] J.B. McMonagel, J.B. Moffat, J. Catal. 91 (1985) 132.
[26] Y. Saito, P.N. Cook, H. Niiyama, E. Echigoya, J. Catal. 95 (1985) 49.
[27] I.K. Song, J.K. Lee, W.Y. Lee, Appl. Catal. A 119 (1994) 107.

[28] Y. Hanada, M. Kamada, K. Umemoto, H. Kominami, Y. Kera, Catal. Lett. 37 (1996) 229.
[29] T. Okuhara, T. Hashimoto, T. Hibi, M. Misono, J. Catal. 93 (1985) 224.
[30] K. Brückman, J.-M. Tatibouët, M. Che, E. Serwicka, J. Haber, J. Catal. 139 (1993) 455.
[31] T. Okuhara, T. Aral, T. Ichiki, K.Y. Lee, M. Misono, J. Mol. Catal. 55 (1989) 293.
[32] J. Bussi, S. Parodi, B. Irigaray, R. Kieffer, Appl. Catal. A 172 (1998) 117.
[33] D. Andriamasinoro, R. Kieffer, A. Kiennemann, J.L. Rehspringer, P. Poix, A. Vallet, J.C. Lavalley, J. Mater. Sci. 24 (1989) 1757.
[34] J. Chunningham, G.H. Al-Sayyed, J.A. Cronin, J.L.G. Fierro, C. Healy, W. Hirschwald, M. Ilyas, J.P. Tobin, J. Catal. 102 (1986) 160.
[35] R.W. McCabe, P.J. Mitchell, J. Catal. 103 (1987) 419.
[36] W. Mokwa, D. Kohl, G. Heiland, Fresenius Z. Anal. Chem. 314 (1983) 315.
[37] D.J.M. Bevan, J.P. Shelton, J.S. Anderson, J. Chem. Soc. (1948) 1729.
[38] S.W. Weller, S.E. Voltz, J. Am. Chem. Soc. 76 (1954) 4695.
[39] V. Krihnasamy, Indian J. Chem. 17A (1979) 437.
[40] D.K. Chakrabarty, K.S. Rane, A.B. Biswas, Indian J. Chem. 15A (1977) 669.
[41] T. Wolkenstein, Adv. Catal. 12 (1960) 189.
[42] A.M. El-Awad, B.M. Abu-Zied, J. Mol. Catal. 176 (2001) 211.
[43] B. Grzybowska-Swierkosz, Mater. Chem. Phys. 17 (1987) 121.
[44] R.B. Fahim, M.I. Zaki, R.M. Gabr, Appl. Catal. 4 (1982) 189.
[45] G. Busca, J. Catal. 120 (1989) 303.
[46] S.R. Ely, R.L. Burwell, J. Colloid Interface Sci. 65 (1978) 244.
[47] R. Hubaut, M. Daage, J.P. Bonnelle, Appl. Catal. 22 (1986) 231.
[48] J. Deren, J. Haber, A. Podgorecka, J. Burzyk, J. Catal. 2 (1963) 161.
[49] C. Zener, Phys. Rev. 82 (1951) 403.
[50] M.I. Zaki, N. Sheppard, J. Catal. 80 (1983) 114.
[51] R.L. Burwell, G.L. Haller, K.C. Taylor, J.F. Read, Adv. Catal. 20 (1969) 1.
[52] D.J. Salley, H. Fehrer, H.S. Taylor, J. Am. Chem. Soc. 63 (1941) 1131.
[53] E.M. Ezzo, N.A. Yosef, H.S. Mazhar, Egypt J. Chem. 27 (1984) 35.
[54] E. Giamello, B. Fubini, M. Bertoldi, G. Busca, A. Vaccari, J. Chem. Soc., Faraday Trans. 1 85 (1989) 237.
[55] B.C. Farzer, P.J. Brown, Phys. Rev. 125 (1962) 1283.
[56] T.A. Egerton, F.S. Stone, J.C. Vickerman, J. Catal. 33 (1974) 299.
[57] D. Scarano, A. Zecchina, A. Reller, Surf. Sci. 198 (1988) 11.
[58] J.C. Kuriacose, C. Daniel, J. Catal. 14 (1969) 77.
[59] L. Nondek, D. Mihajlova, A. Anderav, A. Palazov, M. Kraus, D. Shopov, J. Catal. 40 (1975) 46.
[60] J.C. Kuriacose, C. Daniel, N. Balakrishnan, Indian J. Chem. 7 (1969) 367.
[61] M.L. Cubeiro, J.L. Fierro, J. Catal. 179 (1998) 150.
[62] M. Bertoldi, B. Fubini, E. Giamello, G. Busca, F. Trifiro, A. Vaccari, J. Chem. Soc., Faraday Trans. 1 84 (1988) 1405.
[63] P.J. Miller, G.L. Cessac, R.K. Khanna, Spectochim. Acta 27A (1971) 2019.
[64] F.A. Miller, C.H. Wilkins, Anal. Chem. 24 (1952) 1253.
[65] R.A. Nyquist, R.O. Kagel, Infrared Spectra of Inorganic Compounds, Academic Press, London, 1971, pp. 13–16.
[66] M.I. Zaki, R.B. Fahim, J. Thermal Anal. 31 (1986) 825.
[67] N.E. Fouad, H. Knözinger, M.I. Zaki, S.A.A. Mansour, Z. Phys. Chem. 171 (1991) 75.
[68] J. Haber, Z. Chem. 13 (1973) 24.
[69] W.F. McClune (Ed.), Proceedings of the Joint Committee on Powdered Diffraction Standards, Swarthmore, PA, Powder Diffraction File of Inorganic Compounds, 1983.
[70] Y. Wang, B.H. Davis, Appl. Catal. A 180 (1999) 277.
[71] V. Múèka, Can. J. Chem. 70 (1992) 1914.
[72] J.L. Hutchison, N.A. Briscoe, Ultramicroscopy 18 (1985) 435.
[73] J.D. Lee, Consise Inorganic Chemistra, 5th Edition, Blackwell Scientific Publishers, Hong Kong, 1998, p. 728.
[74] D.R. Lide (Ed. in Chief), CRD Handbook of Chemistry and Physics, 80th Edition, CRC Press, Boca Raton, 1999–2000.
[75] M.H. Yao, R.J. Baird, F.W. Kunz, T.E. Hoost, J. Catal. 166 (1997) 67.
[76] S.V. Tsybulya, G.N. Kryukova, S.N. Goncharova, A.N. Shmakov, B.S. Bal'zhinimaev, J. Catal. 154 (1995) 194.
[77] Y.S. Bhat, J. Das, K.V. Rao, A.B. Halgeri, J. Catal. 159 (1996) 368.
[78] A. Ellison, K.S.W. Sing, J. Chem. Soc., Faraday Trans. 1 74 (1978) 2807.
[79] K.M. Aba El-Salam, Z. Phys. Chem. 95 (1975) 129.
[80] E.I. Odmuah, J.C. Vickerman, J. Catal. 62 (1980) 195.
[81] P. Pomonis, J.C. Vickerman, J. Catal. 55 (1978) 88.
[82] J. Sedláček, M. Kraus, React. Kinet. Catal. Lett. 2 (1975) 27.
[83] D.K. Chakrabarty, D. Guha, I.K. Bhatnagar, A.B. Biswas, J. Catal. 45 (1976) 305.
[84] D.P. McArthur, H. Bliss, J.B. Butt, J. Catal. 132 (1991) 183.
[85] Y.-L. Xiong, L.-T. Weng, P. Bertrand, J. Ladrière, L. Daza, P. Ruiz, B. Delmon, J. Mol. Catal. A 155 (2000) 59.
[86] L.-T. Weng, B. Delmon, Appl. Catal. A 81 (1992) 141.
[87] B. Zhou, T. Machej, P. Ruiz, B. Delmon, J. Catal. 132 (1991) 183.
[88] L.-T. Weng, B. Yasse, J. Ladrière, P. Riuz, B. Delmon, J. Catal. 132 (1991) 343.
[89] S. Harris, R.R. Chianelli, J. Catal. 98 (1986) 17.
[90] S.H. Oh, J.E. Carpenter, J. Catal. 98 (1986) 178.
[91] D.W. Bassett, H.W. Habgood, J. Phys. Chem. 64 (1960) 769.